Research Article

Engineering: Open Access

ISSN: 2993-8643

Design of a Modular Multipoint Electric Vehicle Charging Station Powered by Wind Energy

C. Armenta-Déu* and Jorge C. Reyes

Facultad de Ciencias Físicas. Universidad Complutense de Madrid. 28040 Madrid Spain

***Corresponding Author**
C. Armenta-Déu, Facultad de Ciencias Físicas. Universidad Complutense de Madrid. 28040 Madrid Spain.

Submitted: 2024, Jun 01; **Accepted**: 2024, Jul 04; **Published**: 2024, Jul 11

Citation: Armenta-Déu, C. Reyes, J. C. (2024). Design of a Modular Multipoint Electric Vehicle Charging Station Powered by Wind Energy. *Eng OA, 2*(3), 01-18.

Abstract
The present work focuses on the design of a modular electric vehicle charging station powered by renewable energy, specifically wind energy, for installation on interurban roads. The main objective is to create a sustainable and efficient solution for charging electric vehicles, leveraging natural resources, and reducing dependence on non-renewable energy sources.

We develop a comprehensive analysis of the EV market and their energy demand to design a wind farm for powering the electric vehicle charging station. To achieve this goal, we consider critical factors such as wind speed and other environmental characteristics that influence the efficiency of wind energy generation. We evaluate the design through a study of monthly and hourly coverage, developing an algorithm to simulate the operation of this charging station under current demand conditions.

The modular design of the charging station allows for flexible scalability, adapting to different capacity needs and future expansion. The study concludes that the new design is beneficial not only for the economy but for the environment. We propose a system optimization, considering future technological advancements and possible improvements in integration with the electrical grid and other renewable energy systems.

Keywords: Electric Vehicle, Charging Station, Technology, Modular Design, Wind Farm, Simulation, Sizing

1. Introduction
The electric vehicle implementation in the private and public transportation sectors represents a challenge for our society [1-5]. National and supranational authorities, pushed by the scientific and technical reports warning on the continuous growth of vehicle greenhouse gasses emissions, which contribute to climate warming, are dictating rules addressed to replacing internal combustion engines (ICE) with electric motors [6-9]. In the past year of 2023, a prestigious newspaper, The Economist, published an article saying that electric vehicles could be crucial for the European Union to meet its climate goals, but only if the charging infrastructure is ramped up much faster [10].

Electric vehicle charging stations are a question of economy, technology, and design [11-16]. Car manufacturers develop a specific charging socket to avoid using universal chargers with their brand's vehicles [17-19]. The multiple charging socket type forces the charging station manufacturers to design a complex configuration to give service to the many charger configurations [20-23]. This situation results in higher investment and maintenance costs and the need for larger areas and more complicated designs.

On the other hand, the variable electric vehicle operating voltage, with values between 360 V and 480 V, further complicates, if possible, the charging station design and the energy supply [26-29]. The recent trend of manufacturing electric motors at 800 V operating voltage adds complexity to the already tangled design. A full service to all types of electric vehicles should include different socket types and electric vehicle-matching operating voltage supply. The large combination number of charging configurations reduces the economic viability of a charging station with all options.

Economic profitability is a crucial factor in charging station installation, a factor that makes the owners rarely decide to offer all chances of voltage supply and socket type [30-33]. Since stopping for battery recharge is mandatory when traveling long distances because of the reduced electric vehicle driving range compared to conventional cars, the uncertainty of finding a suitable charging point at any charging station provokes rejection in many drivers when buying an electric vehicle [34-36].

An additional problem derives from the availability of charging points if many vehicles stop at the charging station to refill the battery. Today, time is precious, and drivers search for the minimum delay in charging batteries, especially if they come from the conventional vehicle market powered by internal combustion engines, where refilling a gas tank takes a short time [37-41].

The political measurements to reduce greenhouse gasses (GEI) emissions affect public and private transportation and power generation; in this latter case, power plants progressively abandon fossil fuels in favor of renewable energies [42-44]. Wind energy has become the main contributor to the renewable energy mix due to the on-shore and off-shore installations [45-48].

Connecting wind farms to electric vehicle charging stations reduces grid dependence and contributes to preserving the environment [49-53]. Besides, wind farms operate as distributed generation (DG) power plants, which may work as the principal power supply system for specific applications like electric vehicle charging stations [54,55].

The interconnection between wind farms and electric vehicle charging stations reduces energy losses if located nearby, limits the power load in the electric transportation lines, and lowers reactive power in the network, which requires lower power generation at the power plant [56,57].

Therefore, we should develop a strategy to adapt the charging station to variable operating conditions with minimum changes in the charging point configuration. This paper focuses on this strategy, adopting a modular design for a multipoint charging pole. The design facilitates the charging station enlargement.

2. Fundamentals

This project intends to design a hybrid modular electric vehicle charging station powered by wind energy assisted by batteries. The project goal is to take advantage of both growing markets, wind energy, and electric vehicles, and contribute to a more sustainable future development, promoting clean mobility and reducing fossil fuel dependence.

Pure electric vehicles require a power supply to charge batteries, which depends on the model and driving range [58,59]. The most characteristic parameter regarding the EV power requirement is the battery energy capacity, which defines how much energy a battery contains at full state-of-charge (SOC). This value depends on the battery capacity and operational voltage, as in Equation 1.

$$\xi_{bat} = C_{bat} V_{bat} \quad (1)$$

Battery capacity derives from Equation 1; however, its value depends on charge or discharge rate according to the expression [60].

$$C_{bat} = f_C C_{bat}^o \quad (2)$$

$C_{bat}{}^o$ is the battery nominal capacity for the reference discharge rate, and f_C is the battery capacity correction factor, which is given by [60].

$$f_C = 0.9541 \left(\frac{C_{bat}^o}{I_{bat}} \right)^{0.0148} \quad (3)$$

I_{bat} is the battery charge or discharge current.

The current battery capacity at any state of charge is:

$$C_{bat}^{SOC} = C_{bat} SOC \quad (4)$$

SOC is the battery state-of-charge at any time, which is given by the relation:

$$SOC = \frac{V_{bat}}{V_{bat}^o} \quad (5)$$

V_{bat} is the battery voltage with super-index *o* accounting for the complete state of charge.

Combining equations 1 to 5, we obtain the required energy to charge an electric vehicle battery from a partially or complete discharge state as:

$$\xi_{bat} = 0.9541 \frac{\left(C_{bat}^o \right)^{1.0148}}{I_{bat}^{0.0148}} \frac{V_{bat}^2}{V_{bat}^o} \quad (6)$$

The charging time depends on the current rate and battery voltage at the initial state of the charging process; therefore:

$$t_C = \frac{\xi_{bat}}{I_C V_C} = \frac{0.9541}{I_C V_C} \frac{\left(C_{bat}^o \right)^{1.0148}}{I_{bat}^{0.0148}} \frac{V_{bat}^2}{V_{bat}^o} \quad (7)$$

I_C and V_C are the charging current and voltage. The product $I_C V_C$ represents the required power for battery charging.

3. Electric Vehicle Characteristics

The operational battery voltage has two options: matching the electric motor voltage or using a booster. The first option avoids energy losses in voltage conversion but increases battery stack complexity, cost, and required space for battery placement. The second option involves power losses in voltage conversion at the booster but reduces the space for the battery and the number of battery cells; thus, the investment and replacement cost [61-64].

The interconnection between the electric vehicle and the charging station runs on a specific socket, communicating the car and the charging pole, carrying electric current at the selected voltage and power. Unfortunately, the connecting socket is not normalized; therefore, we can find various types corresponding to different World regions and electric vehicle manufacturers. Four models of connecting sockets are used today in the electric vehicle industry (Figure 1).

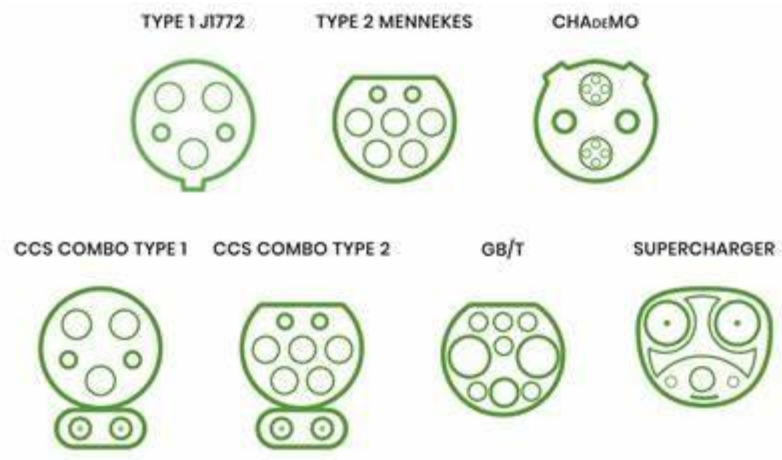

Figure 1: Models of Electric Vehicle Sockets [65].

Electric vehicle sockets may operate at continuous (DC) or alternate current (AC) for variable input voltage, current, and power. Depending on the charging speed, we classify the socket types into two categories: slow and fast charge mode. Tables 1 and 2 show the World region and electric characteristics corresponding to every socket model.

Socket type	J1772		Mennekes	GB/T	Supercharger
World region	Japan	USA	Europe	China	All markets
Maximum power (kW)	1.9	19.2	4-22	7-27.7	7.7-11.5
Input voltage (V)	120	240	250-480	250-400	120/240 – 208/250
Maximum current (A)	16	80	16-32	16-32	16/32 - 48

Table 1: World Region and Characteristics of Electric Vehicle Sockets (Slow Charging Mode) [66].

Socket type	Combo Type 1	Combo Type 2	CHAdeMO	Supercharger	GB/T
World region	USA	Europe	Japan All markets	All markets	China
Maximum power (kW)	150-350	350	50-400	250-350	60-237
Input voltage (V)	200-1000	200-1000	50-1000	300-480	250-950
Maximum current (A)	500	500	400	300	250-400

Table 2: World Region and Characteristics of Electric Vehicle Sockets (Fast Charging Mode) [66].

A second relevant parameter for the electric vehicle characterization is the driving range. Since operating voltage, battery energy capacity, and driving range for electric vehicles depend on the car model, we analyze a group of 363 light-duty and 31 heavy vehicles.

The first part of the study is classifying the vehicle according to the energy capacity; the classification for light-duty and heavy cars corresponds to separate groups as shown in Table 3.

Type of vehicle	Energy capacity (kWh)	Group	%
Light-duty	<30	A	3.0
	30-50	B	15.0
	50-70	C	28.0
	>70	D	54.0
Heavy duty	<200	E	23.4
	>200	F	76.6

Table 3: Electric Vehicle Classification as for the Energy Capacity

The second part of the study corresponds to the operating voltage. According to the literature, the electric vehicle operating voltage distribution is (Table 4) [67].

Type of vehicle	Operating voltage (V)	Group	%
Light-duty	360	A	3.0
	400	B	64.6
	480	C	27.5
	800	D	4.9
Heavy duty	400	E	69.4
	480	F	30.6

Table 4: Electric Vehicle Operating Voltage Distribution

Using data from Table 4, we notice that the most popular voltages are 400 V and 480 V. Nevertheless, if we try to serve all kinds of EVs, we should design a charging station, including all required voltages, no matter the voltage distribution.

4. Wind Farm Power Source

The generated power by a wind turbine derives from the wind speed and wind turbine area according to:

$$P_w = \frac{1}{2} C_p \rho_{air} A u^3 \tag{8}$$

C_p is the power coefficient, which defines the wind turbine efficiency, ρ_{air} is the air density, A is the surface covered by the wind turbine rotor blade, and u is the wind speed.

Considering the mechanic transmission and electricity generation, the wind turbine output power is:

$$P_{out} = \frac{1}{2} C_p \rho_{air} A u^3 \eta_{tr} \eta_{gen} \tag{9}$$

η is the efficiency with sub-indexes *tr* and *gen* for mechanical transmission and electric generator.

Since the wind resource is variable, we must select an appropriate location where wind energy is high enough to cover the charging station's power demand. The selection of the wind farm location depends on the wind resource, which derives from the Weibull distribution (Figure 2). The Weibull distribution shows the probability of occurrence on a wind speed within a specific range. In the case of Figure 2, this range extends to 30 m/s; beyond this point, the wind energy is negligible.

The Y-axis in Figure 2 indicates the relative frequency of any wind speed (X-axis). According to data in Figure 2, the most probable wind speed occurrence is in the 11 to 13 m/s range.

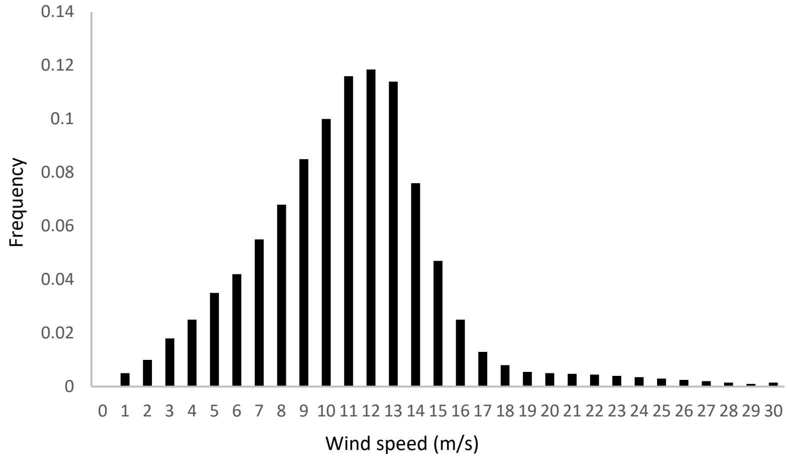

Figure 2: Weibull Distribution

Once the wind resource is known, we size the wind turbine to supply the required power. Considering an average electric generator efficiency of 91% for an output power range between 15 and 25 kW (Figure 3), a transmission efficiency of 94.1%, and a wind turbine efficiency of 40%, the surface power density is [68-70].

$$\frac{P_{out}}{D^2} = (\pi/4)(0.5)(0.4)(1.225)(12^3)(0.941)(0.91) = 284.7\ W/m^2 \qquad (10)$$

D is the wind turbine diameter.

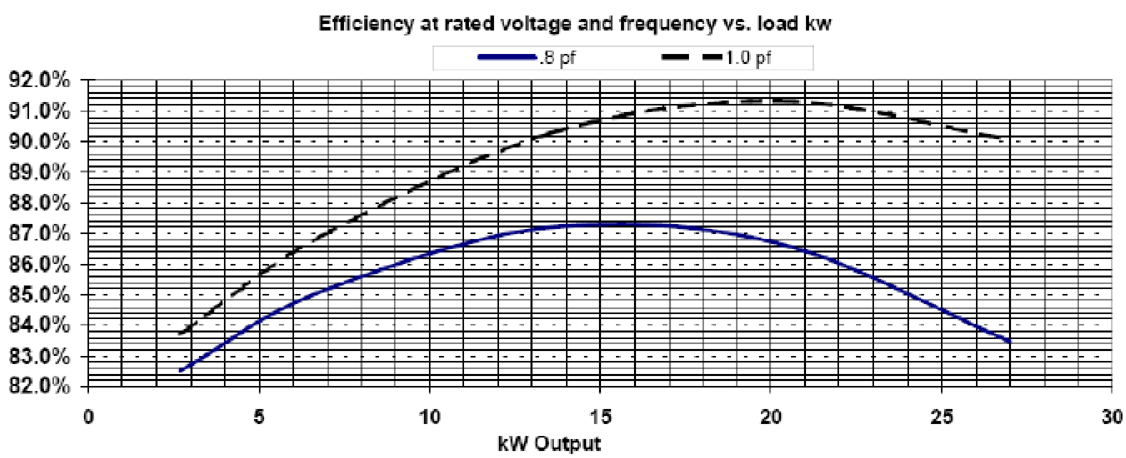

Figure 3: Electric Generator Efficiency

Applying the power density from Equation 10 to a wind turbine diameter between 20 and 40 m, we obtain the following output power (Figure 4):

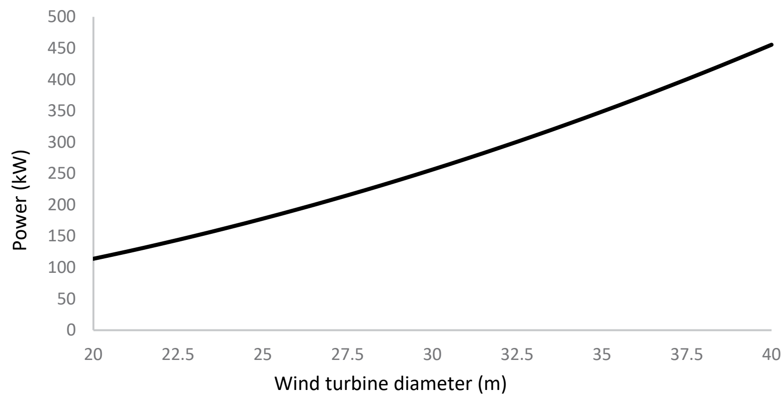

Figure 4: Wind Turbine Output Power vs Rotor Blade Diameter

We observe that, for a 40 m diameter, the wind turbine produces an output power of 455 kW. The number of wind turbines depends on the charging station's energy requirements.

4.1 Engineering Design

The engineering design of the electric vehicle charging station should focus on specific requirements like enough wind energy resources, easy access, available space, and connectivity to the grid. Since we try to provide battery charging service for electric vehicles both on interurban roads or highways with high traffic density and on secondary roads with reduced vehicle circulation, the proposed system has a modular design easily adapted to the needs of the users as well as growing proportionally to the increase in traffic in the location of the charging station.

Based on a modular structure for the charging station, the engineering design consists of a multipoint charging pole, which supplies energy at the selected voltages: 360 V, 400 V, 480 V, and 800 V. The number of charging poles is variable depending on the charging station configuration and the traffic density of the road. We place the charging poles in parallel, as in Figure 5.

The position of the electric vehicle corresponds to the case where the charging connection is at the rear of the vehicle or in the car's rear fin; if the charging connection is located at the front or in the car's front fin, the electric vehicle position reverses. The total area for this configuration is 211 m2. The space dedicated for electric vehicle parking during the charging process is 5 m long and 2.3 m wide, which is enough for a conventional light-duty vehicle. We reserve a 1 m wide aisle for the charging poles and another aisle of 2.5 m width for entering and exiting from the parking space.

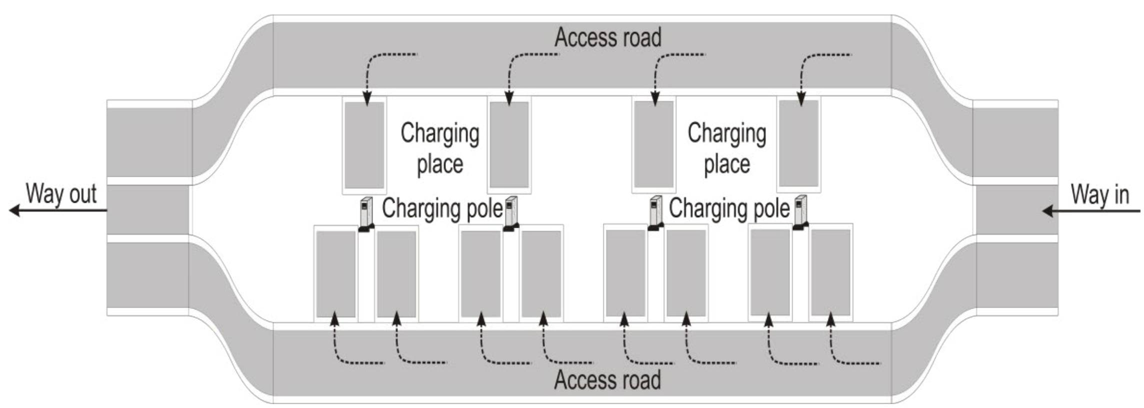

Figure 5: Layout of the Charging Station

The charging station layout includes three charging places for every pole, allowing three electric vehicles to charge simultaneously; therefore, the charging pole configuration should have three sockets with the same or different supplying voltage.

4.2 Charging Pole Configuration

Every charging pole includes three voltage sockets, vertically distributed and with easy access for drivers. The charging pole built-in socket type depends on the World zone to which we manufacture the charging station; the engineering design only includes fast charging sockets: Combo Type 1 for USA and its influencing geographic area, Combo Type 2 for European countries, CHAdeMO for the Japanese market, and GB/T for China and neighboring area. Charging stations specifically built for Tesla models equip charging poles with supercharger sockets. Figure 6 shows the schematic view of a charging pole.

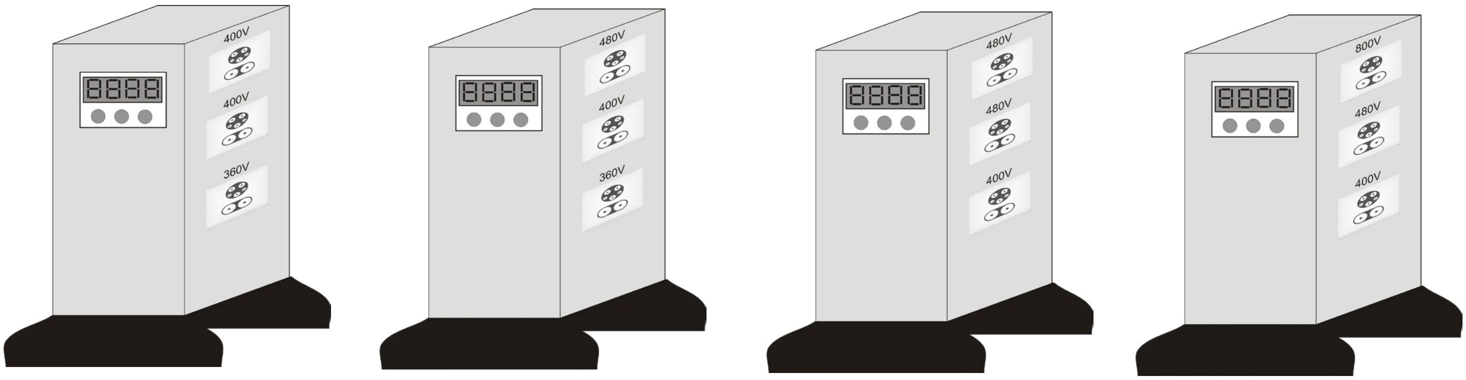

Figure 6: Charging Pole Prototype. Left: Model 1; Center: Model 2; Right: Model 3

Lanes 1, 2, and 3 in Figure 7 equip the charging poles of model 1, while lane 4 equips model 2. This distribution corresponds to the demand voltage by electric vehicle users, with 400 V and 480 V as the most popular and 800 V as the lowest demanded voltage.

Applying the charging pole distribution to the charging station layout, we develop the following engineering design (Figure 7).

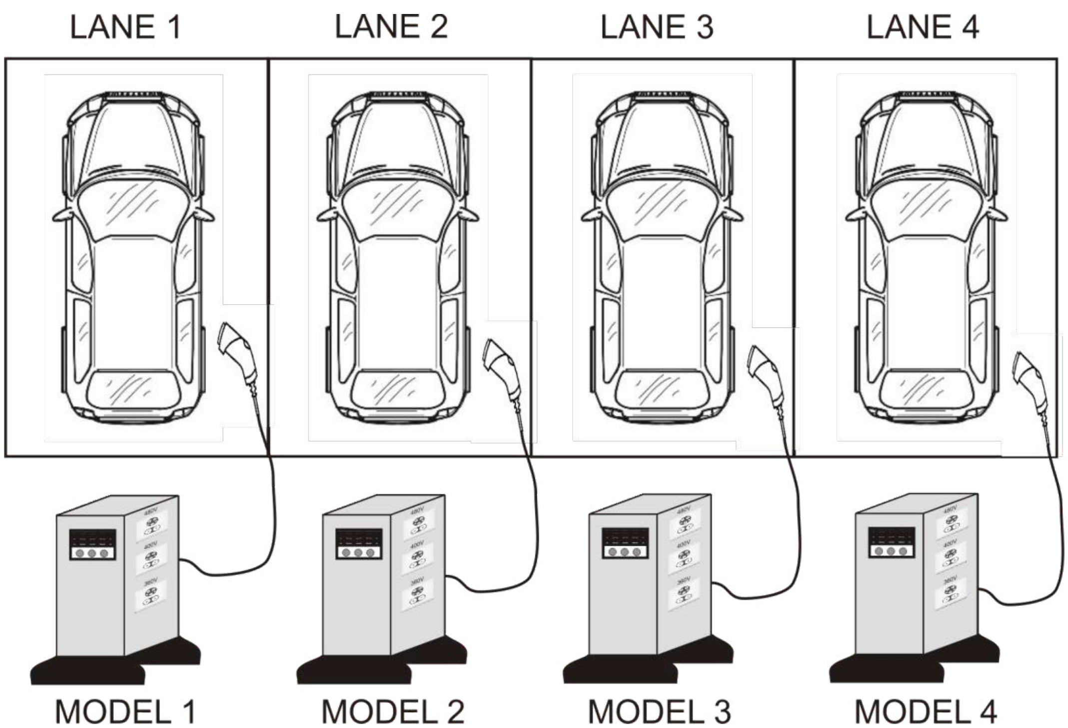

Figure 7: Charging station layout

The socket type on the charging pole corresponds to the World region where the charging station is (USA, Europe, Japan, or China); however, to service imported vehicles with different socket types, we have modified the engineering design, building a double-side charging pole with different socket type on each side (Figure 8).

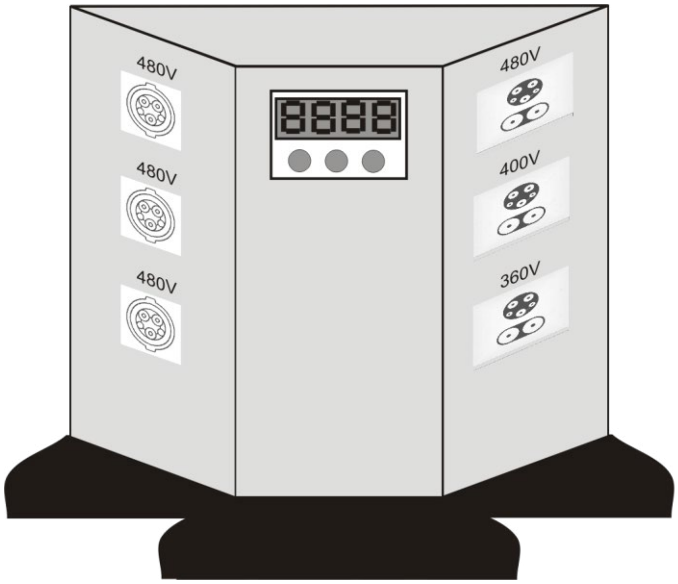

Figure 8: View of the Charging Pole Prototype (Model 5)

4.3 Charging Mode

The charging station provides a configurable charging mode for the users; therefore, the driver can select the charging mode depending on the available time or charge needed. Charging speed depends on battery energy capacity and power supply; nowadays, the power supply ranges from 3.7 kW for domestic uses to 250 kW for public charging stations, which may charge an electric vehicle battery in less than 15 minutes.

In this project, we propose four charging speeds: low, medium, fast, and ultrafast speed, corresponding to a supplying power of 25, 50, 100, and 150 kW. Low charging speed preserves battery health due to the low intake current. Medium charging speed represents a compromise solution between battery health preservation and reduced charging time, and it is probably the most suitable option. Fast and ultrafast charging speed applies to people in a hurry, searching for a minimum delay in a battery charging stop. The ultrafast speed is associated with the highest operating voltage, 800 V.

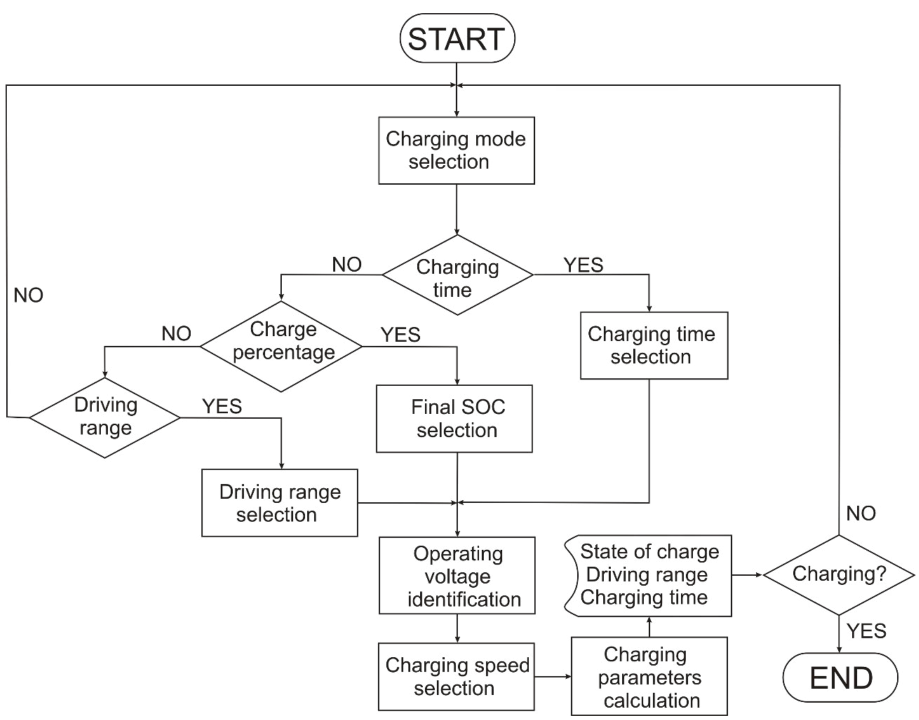

Figure 9: Charging Protocol Flowchart

The charging mode selection by the user is associated with a protocol ruled by an algorithm developed for this project. This protocol pursues to provide the user easy access to practical information and selectable charging options. The developed protocol follows the flowchart shown in Figure 9. The developed protocol offers three options to the user:

• *Mode 1.* The user selects the charging time and speed; the charging pole provides information about the battery state of charge and the electric vehicle driving range at the end of the process

• *Mode 2.* The user selects the supplied charge percentage and the charging speed; the charging pole provides information about the charging time and final battery state of charge

• *Mode 3.* The user selects the driving range after the charging process; the charging pole provides information about the charging time and the final battery state of charge

4.4 Power Demand

Applying the charging station layout shown in Figure 5 and the charging pole configuration from Figure 6, we have 12 sockets distributed in the following way: two for 360 V, five for 400 V, 4 for 480 V, and one for 800 V. The power associated with every socket derives from the charging time and electric vehicle battery capacity. Since people arriving at a charging station on an interurban road or a highway look for a fast charge, we estimate the minimum charging time for a full charge depending on battery energy capacity and socket power supply (Table 5). The electric vehicle operating voltage relates to the battery energy capacity; for our case, the relation is 48 kWh for 360 V, 64 kWh for 400 V, 92 kWh for 480 V, and 120 kWh for 800 V.

	Battery energy capacity (kWh)			
Socket power supply (kW)	***48***	***64***	***92***	***120***
50	58	77	110	144
65	44	59	85	111
90	32	40	61	80
120	24	32	46	60

Table 5: Estimated Time (Min) for Battery Fully Charge [71].

We determine the battery capacity using the relation:

$$C_{bat} = \frac{\xi_{bat}}{V_{op}} \quad (11)$$

ξ_{bat} is the battery energy capacity, and V_{op} is the operating voltage.

Applying the setup values for the various operating voltages, we obtain:

$$\begin{aligned} C_{bat}^{360} &= \frac{48000}{360} = 133.3\ Ah\,;\ C_{bat}^{400} = \frac{64000}{400} = 160\ Ah \\ C_{bat}^{480} &= \frac{92000}{480} = 191.7\ Ah\,;\ C_{bat}^{800} = \frac{120000}{800} = 150\ Ah \end{aligned} \quad (12)$$

Because the charging sockets are all of the fast charging type, the charge current is:

$$\begin{aligned} I_C^{360} &= \frac{133.3}{(58/60)} = 138\ A\,;\ I_C^{400} = \frac{160}{(77/60)} = 125\ A \\ I_C^{480} &= \frac{191.7}{(85/60)} = 135A\,;\ I_C^{800} = \frac{150}{(60/60)} = 150\ A \end{aligned} \quad (13)$$

Therefore, the socket power is:

$$\begin{aligned} P_1^{360} &= (138)(360) = 50\ kW\,;\ P_2^{400} = (125)(400) = 50\ kW \\ P_3^{480} &= (135)(480) = 65\ kW\,;\ P_4^{800} = (150)(800) = 120\ kW \end{aligned} \quad (14)$$

Computing all sockets, the maximum required power if all sockets operate simultaneously is:

$$P_T = (2)(50) + (5)(50) + (4)(65) + (1)(120) = 730\ kW \quad (15)$$

Energy demand depends on charging station coverage factor and socket usage time. Assuming a 75% coverage factor during day hours and 25% at nighttime, which is a consistent value for a highway or interurban charging station, the daily energy demand is:

$$\xi_{ch-st} = (0.75)(12)(730) + (0.25)(12)(730) = 8760\ kWh \quad (16)$$

The energy value in Equation 16 corresponds to a monthly energy demand of 262.8 MWh, considering 30 days per month and daily constant use of the charging station.

4.5 Wind Farm

The wind farm design and sizing depend on the wind resource and power demand from the charging station. We base the calculation of this latter parameter on a critical power demand for sixteen working hours per day and a coverage factor of 75%. We define the coverage factor as the ratio of charging poles' operational time over the global daily time; in our case, the coverage factor corresponds to 12 hours. On the other hand, the average power demand during electric vehicle charging is 150 kW, applying statistical analysis to the charging poles; applying these values, we obtain a daily energy demand of 1800 kWh per charging pole, equivalent to 21696 kWh for the charging station [72].

Since the energy demand is moderate, we select intermediate wind turbines in the 500 kW to 1 MW range, with a 660 kW power turbine according to wind resource and wind turbine diameter [73]. The selected model is VESTAS V47 [74]. Table 5 shows the technical characteristics of the wind turbine.

Parameter	***Value***
Nominal power	660 kW
Starting wind speed	4 m/s
Max. power wind speed	15 m/s
Cut-off wind speed	25 m/s
Diameter	47 m
Hub height	50 m

Table 5: Wind Turbine Technical Characteristics

Using this wind turbine type, the wind farm consists of 2 turbines to supply a global power of 1320 kW, representing 1.8 times more power than required at the peak point charging station. The surplus of 80% in power supply is necessary since the wind farm does not supply the maximum power continuously.

Figure 10 shows the power curve corresponding to the wind turbine.

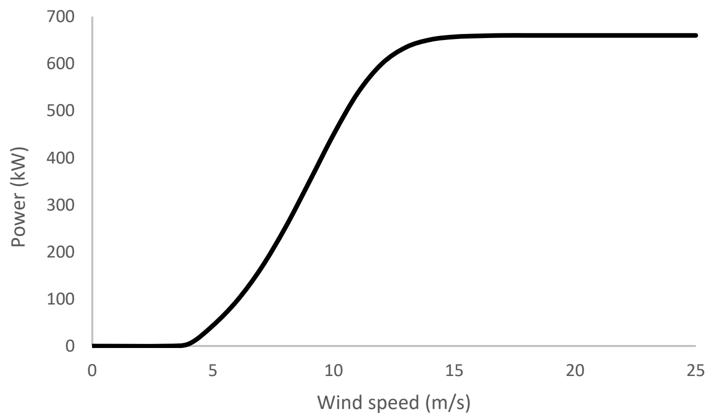

Figure 10: VESTAS V47 Wind Turbine Power Curve

Using data from the New European Wind Atlas, we determine the statistical parameters regarding the wind resource. Figure 11 shows the results of the database statistical treatment for the monthly evolution [75].

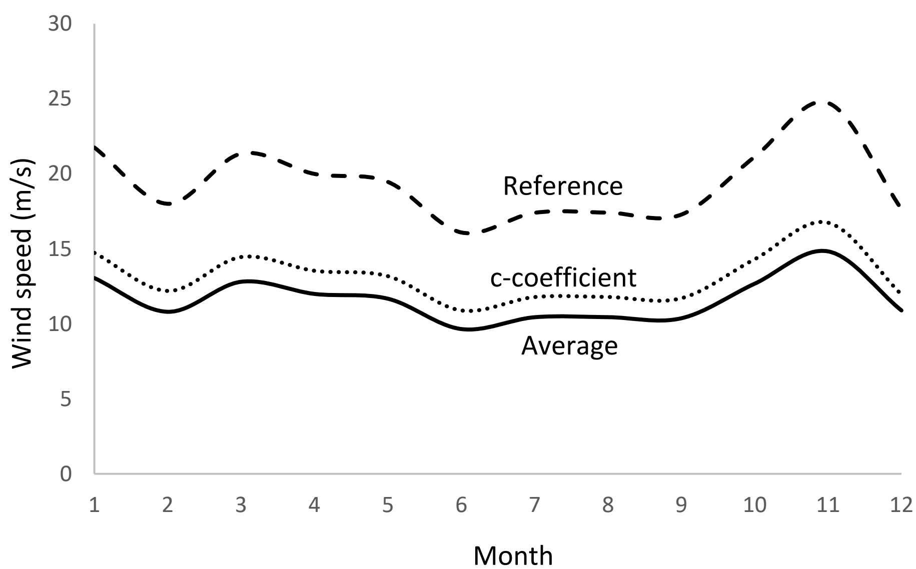

Figure 11: Wind Resource Monthly Evolution for the Selected Location

Averaging over the whole year, we obtain the following results:

Month	Average wind speed (m/s)	σ_{av}	Reference wind speed (m/s)	*k*	*c*
Year→	**11.64**	**1.9973**	**19.35**	**2.1454**	**13.10**

Table 6: Statistical Results of the Monthly Wind Energy Resource

We notice that the yearly average wind speed matches the peak value in Figure 2 by 97%. Besides, the year average standard deviation, σ_{av}, is near 2, meaning that the wind speed distribution concentrates around a center value, which favors a good wind farm design. On the other hand, the average to the reference wind speed is 0.60, which indicates that the performance of the wind resource is near ideal (R=0.593).

Regarding Weibull coefficients, *k*, and *c*, we realize the wind speed distribution behaves as a Rayleigh one ($k = 2$), meaning that around the wind speed peak value, the wind speed distribution is symmetric, which minimizes the calculation and improves accuracy in power determination. The c-coefficient to average wind speed ratio, $c/u_{av} = 1.125$, is in the range for a good wind speed distribution ($1 < c/u_{av} < 1.15$).

Repeating the calculation for the hourly distribution, we obtain (Figure 12). Averaging over the day, we have the following results:

Month	Average wind speed (m/s)	σ_{av}	Reference wind speed (m/s)	*k*	*c*
Year→	**11.62**	**2.1226**	**19.35**	**2.1454**	**13.10**

Table 7: Statistical Results of the Hourly Wind Energy Resource

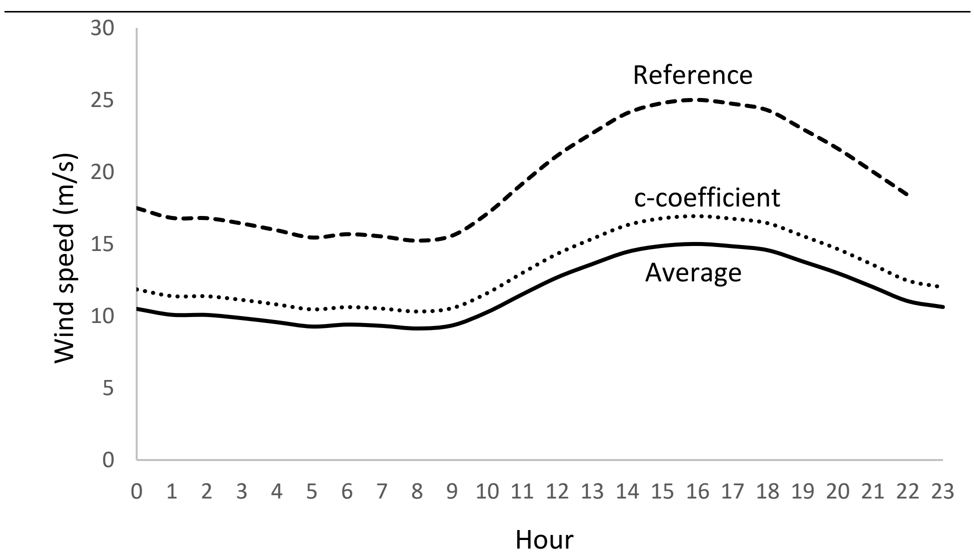

Figure 12: Wind Resource Daily Evolution for the Selected Location

As in the case of monthly evolution, the average wind speed matches the peak value in Figure 2 by 96.8%. Likewise, the standard deviation remains low, with a value near 2, proving that the daily wind speed distribution concentrates around a centered value.

From the statistical analysis, we calculate the average daily and monthly energy generation over the year by multiplying the speed bin from the wind speed frequency curve by the corresponding power value from the power wind turbine curve. The sum of the generated energy for every speed bin provides the global energy generation. Figure 13 and Table 7 show the monthly energy generation and coverage factor, while Figure 14 and Table 8 account for the daily case.

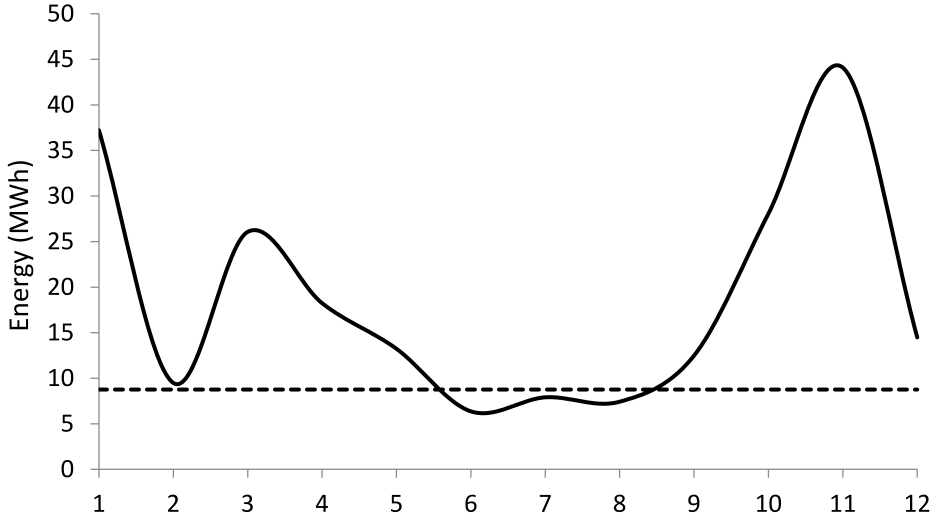

Figure 13: Wind Farm Daily Energy Generation

Dashed line in Figure 13 represents the average daily energy consumption in the charging station.

Month	January	February	March	April	May	June
CF (%)	107.7	27.5	75.4	52.8	38.3	18.4
Month	July	August	September	October	November	December
CF (%)	22.9	21.5	36.1	81.2	127.6	41.9

Table 8: Wind Energy Monthly Coverage Factor (CF)

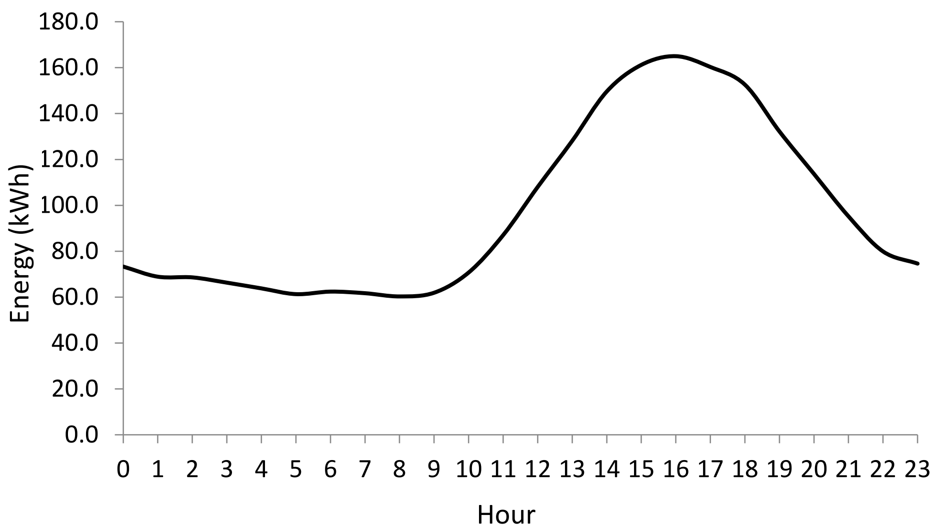

Figure 14: Wind Farm Hourly Energy Generation

Hour	0	1	2	3	4	5	6	7	8	9	10	11
CF (%)	30.5	28.6	28.6	27.6	26.6	25.6	26.0	25.7	25.1	25.8	29.4	36.3
Hour	12	13	14	15	16	17	18	19	20	21	22	23
CF (%)	45.0	53.4	62.3	67.2	68.7	66.8	63.4	55.1	47.4	39.7	33.3	31.1

Table 9: Wind Energy Daily Coverage Factor (CF)

Computing data from Figure 13 over the entire year, we obtain an average monthly wind energy generation of 18.756 MWh per day, which exceeds the charging station demand by a factor of 1.14, enough to cover electric vehicle charging in a year.

Nevertheless, in June, July, and August, the wind energy supply does not cover the charging station needs, which requires an external power supply from the grid. An alternative to the grid connection is storing the excess energy during months when wind energy generation exceeds charging station demand in batteries. Since the energy surplus is high, this solution is not economically reliable because of the high battery size and the associated cost.

In case the electric vehicle charging station operates disconnected from the grid, the battery size should have the following energy capacity:

$$\xi_{bat} = \sum_{i=1}^{12} \left(\xi_{ch-st} - \xi_{wind} \right)^{+} \tag{17}$$

The superscript "+" indicates that we consider only the months when the charging station energy demand overpasses the wind farm energy supply.

Replacing data, we have:

$$\xi_{bat} = 4.58MWh \tag{18}$$

Considering the battery operates at 400 V to match the most common operating voltage for electric vehicle charging, the battery capacity is:

$$C_{bat} = \frac{4.58x10^{6}}{400} = 11450Ah \tag{19}$$

5. Electric Engineering

Since the wind turbines supply alternate current at 690 VAC, we operate at intermediate high voltage, 24kV, to reduce transmission losses. The first step of the electric engineering design is converting 690 VAC to 24 VAC (Figure 15).

Operating at 24 kV in the transmission line saves a significant amount of energy, which depends on the distance between the wind farm and the charging station. Keeping the minimum distance established by international normative for safety reasons, which is set up at 500 m, and considering a cooper wiring of appropriate diameter for the carrying current, the power losses are [76].

$$\dot{\xi}_{L} = I_{tr}^{2} R = I_{tr}^{2} \frac{\rho_{wr} L_{wr}}{S_{wr}} \tag{20}$$

V_{tr} is the transmission line voltage and ρ_{wr}, S_{wr}, and L_{wr} are the wiring resistivity, section and length, respectively.

Retrieving data from technical datasheet [77].

$$\begin{aligned} \xi_{L}^{24kV} &= \left(\frac{2x660x10^{3}}{24x10^{3}} \right)^{2} \frac{\left(1.68x10^{-8}\right)\left(500\right)}{\left(16x10^{-6}\right)} = 1588\,W \\ \xi_{L}^{690V} &= \left(\frac{2x660x10^{3}}{690} \right)^{2} \frac{\left(1.68x10^{-8}\right)\left(500\right)}{\left(16x10^{-6}\right)} = 1.92\ MW \end{aligned} \tag{21}$$

It is evident that operating at 690 V in the transmission line is energy wasting.

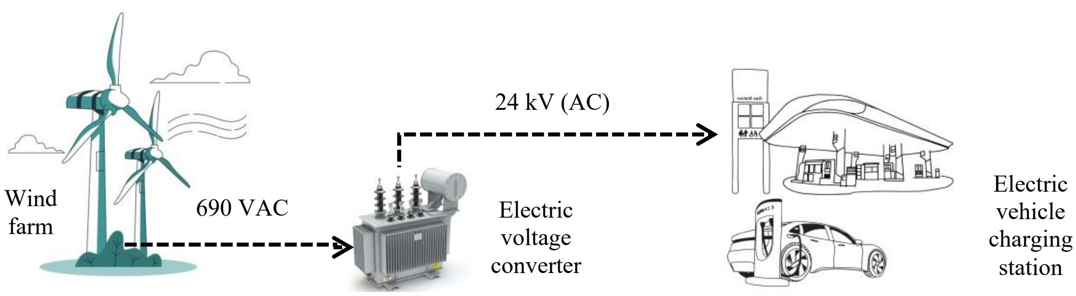

Figure 15: Layout of Voltage Conversion Line

The second step of the voltage conversion line is adapting the high voltage from the transmission line to the working voltage at the charging station. Two architecture voltage conversions arise: lowering the high voltage to every servicing voltage at the charging pole or reducing the voltage from 24 kV to a low operative value and converting this low voltage to every socket voltage.

Analyzing the two architectures, we propose a voltage drop from 24 kV to 400 V since this is the most used working voltage in electric vehicles. The proposed system uses two AC/DC voltage converters to have a redundant power supply in case of failure. With this architecture, we guarantee a constant service even if one of the conversion systems fails. The proposed architecture also saves money since it reduces the number of voltage converters, as in the case of individual conversion for every socket voltage.

The voltage conversion system has a principal converter from 24 kV to 400 V and three secondary converters: the first from 400 V to 360 V, the second from 400 V to 480 V, and the third from 400 V to 800 V. As already mentioned, an auxiliary converter from 24 kV to 400 V remains in standby mode as a safety power supply in case of failure of the principal converter (Figure 16).

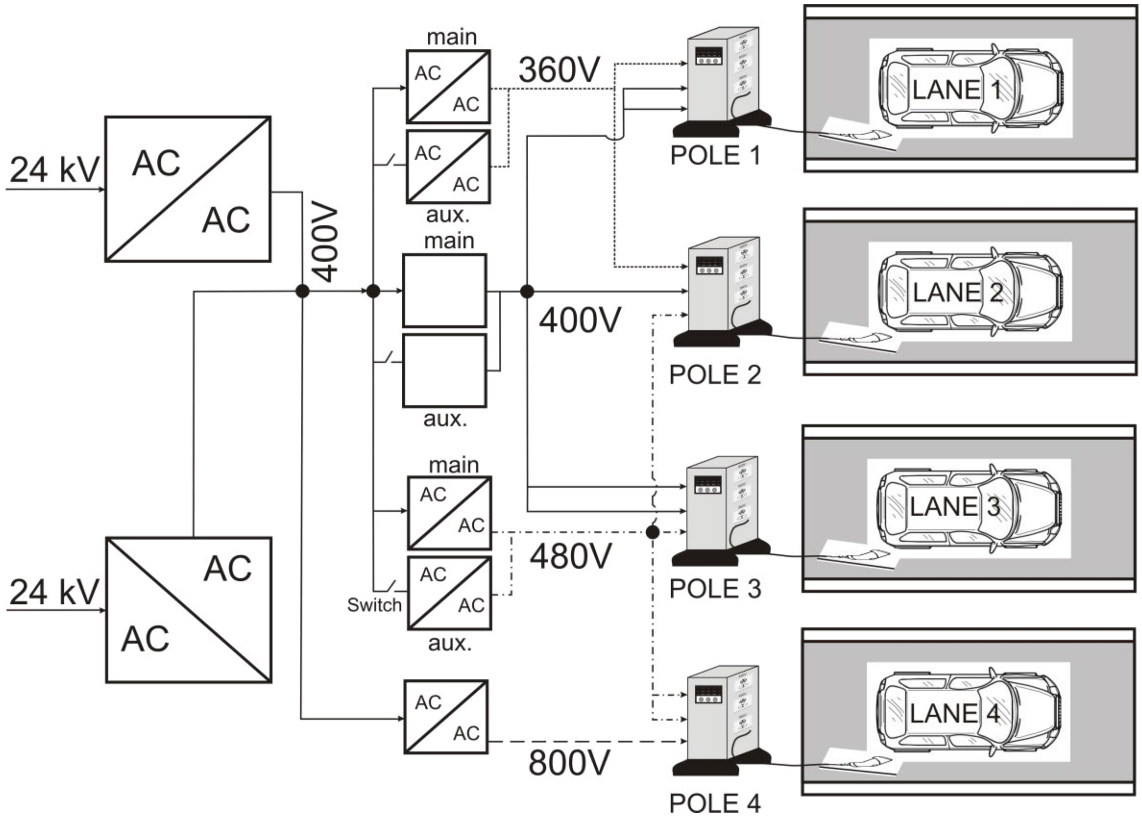

Figure 16: Electric Wiring and Voltage Conversion

The engineering design of the voltage conversion system also duplicates the intermediate voltage converters to warranty the constant power source to the charging poles; the only socket with no redundant voltage converter is the 800 V since the low number of electric vehicles equipping this configuration does not justify the voltage converter duplication.

In current conditions, the main voltage converter operates with the auxiliary one in standby mode; if the main voltage converter fails, the switch closes, and the power is derived to the auxiliary one, supplying power to the charging pole and warrantying electric vehicle charge service.

6. Operational Protocol

We have developed a protocol that controls the charging station's operational mode. The protocol simulates the energy demand at the charging station when arriving at electric vehicles; the protocol works with variable battery states of charge, various voltages, and different charging modes to simulate current conditions. The goal of the protocol is to reproduce the living conditions in any electric vehicle charging station around the World with high accuracy.

The protocol parametrizes the operating conditions like electric vehicle voltage, battery energy capacity and state of charge, charging mode, ultrafast, fast, medium or slow, charging time, expected driving range, etc. The advantage of parametrizing the operational mode of the charging station through specific algorithms is the applicability of the developed protocol to almost any charging station and working conditions.

The protocol code includes three steps: in the first one, the system defines the characteristic parameters of the charging station, which are:

- Day hours: Corresponds to the daily working time; in our case 16 hours
- Porct Charge: This is the charge percentage or battery state-of-charge at the end of the charging process, selected by the user. The available range is 20% to 80%, corresponding to the charging mode 2. The user selects a value within the specific range provided by the protocol
- Consumption: Corresponds to the electric vehicle energy consumption rate in Wh/km. The protocol gives three options to the driver: 135 Wh/km, 160 Wh/km, and 210 Wh/km, corresponding to a low rate for light-duty vehicles, a medium rate for SUVs and similar vehicles, and a high rate for heavy vehicles. The driver must select one of the options according to the vehicle type.
- Driving range: Defines the traveling distance the driver wants after charging the battery. The selectable range is 25 km to 250 km in a 25 km step. Corresponds to charging mode 3
- tCharge: It is the available time for charging the electric vehicle. It is configured from 20 minutes to 2.5 hours in 10 minutes step. Corresponds to charging mode 1

- ChargeMode: Vector which defines the charging mode

In the second step, the protocol collects information about the vehicle when connected to the charging pole. The collected information is the battery voltage, state of charge, and energy capacity.

In the third and final step, the protocol calculates the required energy to charge the battery according to the provided information in the previous steps. The protocol code simulates the charging process for the voltage and charge rate defined configuration for the four charging poles. The protocol determines the number of used sockets, checking the charging station coverage factor (CF) database, which provides the CF value as a function of the day hour. The process supplies the operating time (hOper).

The protocol develops the following procedure for every charging pole and socket:

- The program randomly selects an operating voltage (VBati) using the tool "randi"
- Depending on the voltage the program randomly selects a charging rate (ChSpeed). The following restrictions to the charging rate apply: Ultrafast charging is not allowed for low operating voltage (360V), and low charging rate is not allowed for ultrahigh operating voltage (800V) neither
- The program runs a loop"while" until the cumulative socket operating time exceeds the setup value (hOper). The protocol code randomly executes one of the charging modes (Mode1; Mode2; Mode3) within the loop. Every mode returns the operating time and the energy consumption, which are stored as program variable data (Energy, time, Mode) in kWh, hours, and mode type (1,2, or 3)
- At the end of the loop, if time exceeds the hOper value, the protocol code adjusts the energy and time vectors to match the operating time
- The protocol calculates the global required energy by adding the daily energy consumption for every charging pole (TotDem)
- The code determines the monthly and daily wind energy generation, checking the wind turbine power curve and Weibull distribution from the wind energy system database
- The protocol calculates the yearly operating time (HAY) from the Weibull distribution and daily and monthly hours to determine year and monthly wind energy generation
- The program calculates the coverage of energy requirement with wind energy as a percentage by comparing the generation of a typical day for each month of the year and the hourly generation with the total demand and the demand adjusted for the hours of operation, respectively

7. Conclusions

The renewable supply systems implementation in electric stations has numerous benefits, including reducing dependence on fossil fuels and reducing the carbon footprint. Renewable energy sources adoption can also improve energy resilience, offering a more stable and secure supply in the face of fluctuations in fossil fuel prices and supply disruptions.

This work manages to design an electric vehicle charging station powered by renewable energy, specifically wind energy, demonstrating the viability and effectiveness of integrating sustainable energy sources into mobility electrical infrastructures. We develop a modular and scalable design through a detailed analysis of the market context and environmental conditions; the developed system adapts to various capacity needs and future expansion. In addition, we build simulation tools and algorithms that not only validate the system performance under current demand conditions but can also be used to optimize the design of future projects, providing a solid basis for the sustainable energy infrastructures planning and design.

These advances reduce carbon emissions and promote energy independence and efficient use of natural resources, setting a precedent for future innovations in the electric mobility field and renewable energy applications.

References

1. Masson-Delmotte, V., Zhai, P., Pörtner, H. O., Roberts, D., Skea, J., Shukla, P. R., ... & Waterfield, T. (2019). Global warming of 1.5 C. *An IPCC Special Report on the impacts of global warming of, 1*, 93-174.
2. Chhetri, A. B., & Zatzman, G. (2008). Global Warming-A Technical Note. *Nature Science and Sustainable Technology Research Progress, 323.*
3. Khandekar, M. L., Murty, T. S., & Chittibabu, P. (2005). The global warming debate: A review of the state of science. *Pure and Applied Geophysics, 162,* 1557-1586.
4. Masson-Delmotte, V., Zhai, P., Pörtner, H. O., Roberts, D., Skea, J., & Shukla, P. R. (2022). *Global Warming of 1.5 C: IPCC special report on impacts of global warming of 1.5 C above pre-industrial levels in context of strengthening response to climate change, sustainable development, and efforts to eradicate poverty.* Cambridge University Press.
5. Verheggen, B., Strengers, B., Cook, J., Van Dorland, R., Vringer, K., Peters, J., ... & Meyer, L. (2014). Scientists' views about attribution of global warming. *Environmental science & technology, 48*(16), 8963-8971.
6. Mačiulis, P., Konstantinavičiutė, I., & Pilinkienė, V. (2018). Assessment of electric vehicles promotion measures at the national and local administrative levels. *Engineering Economics, 29*(4), 434-445.
7. Begley, J., Berkeley, N., Donnelly, T., & Jarvis, D. (2016). National policy-making and the promotion of electric vehicles. *International Journal of Automotive Technology and Management, 16*(3), 319-340.
8. Obrecht, M., Fale, M., Muneer, T., & Knez, M. (2018). Review of policies for promotion of electric vehicles. *Production Engineering Archives, 21*(21), 28-31.
9. Martins, H., Henriques, C. O., Figueira, J. R., Silva, C. S., & Costa, A. S. (2023). Assessing policy interventions to

stimulate the transition of electric vehicle technology in the European Union. *Socio-Economic Planning Sciences, 87*, 101505.
10. Electric vehicles could be crucial for the EU to meet its climate goals. The Economist. May 22nd, 2023 Berlin
11. Xiang, Y., Liu, J., Li, R., Li, F., Gu, C., & Tang, S. (2016). Economic planning of electric vehicle charging stations considering traffic constraints and load profile templates. *Applied Energy, 178,* 647-659.
12. Shuai, W., Maillé, P., & Pelov, A. (2016). Charging electric vehicles in the smart city: A survey of economy-driven approaches. *IEEE Transactions on Intelligent Transportation Systems, 17*(8), 2089-2106.
13. Yan, Q., Dong, H., & Zhang, M. (2021). Service evaluation of electric vehicle charging station: An application of improved matter-element extension method. *Sustainability, 13*(14), 7910.
14. Center, F. S. E., & Kettles, J. D. (2015). Electric vehicle charging technology analysis and standards.
15. Sachan, S., Deb, S., Singh, P. P., Alam, M. S., & Shariff, S. M. (2022). A comprehensive review of standards and best practices for utility grid integration with electric vehicle charging stations. *Wiley Interdisciplinary Reviews: Energy and Environment, 11*(3), e424.
16. Nezamuddin, O. N., Nicholas, C. L., & dos Santos, E. C. (2021). The problem of electric vehicle charging: State-of-the-art and an innovative solution. *IEEE Transactions on Intelligent Transportation Systems, 23*(5), 4663-4673.
17. Hafez, O., & Bhattacharya, K. (2017). Optimal design of electric vehicle charging stations considering various energy resources. *Renewable energy, 107*, 576-589.
18. Schmidt, M., Zmuda-Trzebiatowski, P., Kiciński, M., Sawicki, P., & Lasak, K. (2021). Multiple-criteria-based electric vehicle charging infrastructure design problem. *Energies, 14*(11), 3214.
19. Hu, D., Zhang, J., & Zhang, Q. (2019). Optimization design of electric vehicle charging stations based on the forecasting data with service balance consideration. *Applied soft computing, 75,* 215-226.
20. Ricaud, C., & Vollet, P. (2010). Connection system on the recharging spot–a key element for electric vehicles. *Schneider Electric.*
21. Raff, R., Golub, V., Pelin, D., & Topić, D. (2019, July). Overview of charging modes and connectors for the electric vehicles. In *2019 7th International Youth Conference on Energy (IYCE)* (pp. 1-6). IEEE.
22. EV Charging Connector Types: What You Need to Know. Wallbox. [Accessed online: 14/06/2024]
23. EV Charging Connector Types: A Complete Guide. Electric Vehicle Energy Storage Company (EVESCO). Power Sony Corporation. [Accessed online: 14/06/2024]
24. Rajendran, G., Vaithilingam, C. A., Misron, N., Naidu, K., & Ahmed, M. R. (2021). A comprehensive review on system architecture and international standards for electric vehicle charging stations. *Journal of Energy Storage, 42,* 103099.
25. Bakker, S., & Trip, J. J. (2015). An analysis of the standardization process of electric vehicle recharging systems. *E-Mobility in Europe: Trends and Good Practice*, 55-71.
26. Rajendran, G., Vaithilingam, C. A., Misron, N., Naidu, K., & Ahmed, M. R. (2021). Voltage oriented controller based vienna rectifier for electric vehicle charging stations. *IEEE Access, 9,* 50798-50809.
27. Minesawa, R., Ochiai, Y., Ishida, S. Market and Technology Trends for EV Charging Stations. Renesas Electronic Corporation. Published: June 26, 2023 [Accessed online: 14/06/2024]
28. EV Charging Basics. EV Charging Resources. CALeVIP. California Energy Commission. [Accessed online: 14/06/2024]
29. Chakraborty, S., Vu, H. N., Hasan, M. M., Tran, D. D., Baghdadi, M. E., & Hegazy, O. (2019). DC-DC converter topologies for electric vehicles, plug-in hybrid electric vehicles and fast charging stations: State of the art and future trends. *Energies, 12*(8), 1569.
30. Mercan, M. C., Kayalica, M. Ö., Kayakutlu, G., & Ercan, S. (2020). Economic model for an electric vehicle charging station with v ehicle-to-grid functionality. *International Journal of Energy Research, 44*(8), 6697-6708.
31. Schroeder, A., & Traber, T. (2012). The economics of fast charging infrastructure for electric vehicles. *Energy Policy, 43,* 136-144.
32. Hecht, C., Figgener, J., & Sauer, D. U. (2022). Analysis of electric vehicle charging station usage and profitability in Germany based on empirical data. *Iscience, 25*(12).
33. Alhazmi, Y. A., & Salama, M. M. (2017). Economical staging plan for implementing electric vehicle charging stations. *Sustainable Energy, Grids and Networks, 10,* 12-25.
34. White, L. V., Carrel, A. L., Shi, W., & Sintov, N. D. (2022). Why are charging stations associated with electric vehicle adoption? Untangling effects in three United States metropolitan areas. *Energy Research & Social Science, 89*, 102663.
35. Globisch, J., Plötz, P., Dütschke, E., & Wietschel, M. (2019). Consumer preferences for public charging infrastructure for electric vehicles. *Transport Policy, 81*, 54-63.
36. Wolbertus, R., Kroesen, M., van den Hoed, R., & Chorus, C. G. (2018). Policy effects on charging behaviour of electric vehicle owners and on purchase intentions of prospective owners: Natural and stated choice experiments. *Transportation Research Part D: Transport and Environment, 62,* 283-297.
37. Wang, Q. J., Feng, G. F., Wang, H. J., & Chang, C. P. (2022). The influence of political ideology on greenhouse gas emissions. *Global Environmental Change, 74,* 102496.
38. Poudenx, P. (2008). The effect of transportation policies on energy consumption and greenhouse gas emission from urban passenger transportation. *Transportation Research Part A: Policy and Practice, 42*(6), 901-909.
39. Hensher, D. A. (2008). Climate change, enhanced greenhouse gas emissions and passenger transport–What can we do to make a difference?. *Transportation Research Part D: Transport and Environment, 13*(2), 95-111.
40. Kenworth, J. (2003). Transport energy use and greenhouse

gases in urban passenger transport systems: A study of 84 global cities.
41. Shaheen, S. A., & Lipman, T. E. (2007). Reducing greenhouse emissions and fuel consumption: Sustainable approaches for surface transportation. *IATSS research, 31*(1), 6-20.
42. Sims, R. E., Rogner, H. H., & Gregory, K. (2003). Carbon emission and mitigation cost comparisons between fossil fuel, nuclear and renewable energy resources for electricity generation. *Energy policy, 31*(13), 1315-1326.
43. Holechek, J. L., Geli, H. M., Sawalhah, M. N., & Valdez, R. (2022). A global assessment: can renewable energy replace fossil fuels by 2050?. *Sustainability, 14*(8), 4792.
44. Lima, M. A., Mendes, L. F. R., Mothé, G. A., Linhares, F. G., De Castro, M. P. P., Da Silva, M. G., & Sthel, M. S. (2020). Renewable energy in reducing greenhouse gas emissions: Reaching the goals of the Paris agreement in Brazil. *Environmental Development, 33*, 100504.
45. Ramírez, F. J., Honrubia-Escribano, A., Gómez-Lázaro, E., & Pham, D. T. (2018). The role of wind energy production in addressing the European renewable energy targets: The case of Spain. *Journal of Cleaner Production, 196*, 1198-1212.
46. Zubi, G., Bernal-Agustín, J. L., & Marín, A. B. F. (2009). Wind energy (30%) in the Spanish power mix—technically feasible and economically reasonable. *Energy Policy, 37*(8), 3221-3226.
47. Sadorsky, P. (2021). Wind energy for sustainable development: Driving factors and future outlook. *Journal of Cleaner Production, 289,* 125779.
48. Haidi, T., & Cheddadi, B. (2022). State of wind energy in the world: evolution, impacts and perspectives. *Int. J. Tech. Phys. Probl. Eng, 41,* 347-352.
49. Noman, F., Alkahtani, A. A., Agelidis, V., Tiong, K. S., Alkawsi, G., & Ekanayake, J. (2020). Wind-energy-powered electric vehicle charging stations: Resource availability data analysis. *Applied Sciences, 10*(16), 5654.
50. Fathabadi, H. (2017). Novel wind powered electric vehicle charging station with vehicle-to-grid (V2G) connection capability. *Energy conversion and management, 136*, 229-239.
51. Chellaswamy, C., Nagaraju, V., & Muthammal, R. (2018). Solar and wind energy based charging station for electric vehicles. *International Journal of Advanced Research in Electrical, Electronics and Instrumentation Engineering, 7*(1), 313-324.
52. Li, H., Liu, H., Ji, A., Li, F., & Jia, Y. (2013, August). Design of a hybrid solar-wind powered charging station for electric vehicles. In *2013 international conference on materials for renewable energy and environment* (Vol. 3, pp. 977-981). IEEE.
53. Alkawsi, G., Baashar, Y., Abbas U, D., Alkahtani, A. A., & Tiong, S. K. (2021). Review of renewable energy-based charging infrastructure for electric vehicles. *Applied Sciences, 11*(9), 3847.
54. Aldhanhani, T., Al-Durra, A., & El-Saadany, E. F. (2017, December). Optimal design of electric vehicle charging stations integrated with renewable DG. In *2017 IEEE Innovative Smart Grid Technologies-Asia (ISGT-Asia)* (pp. 1-6). IEEE.
55. Ahadi, A., Sarma, S., Moon, J. S., Kang, S., & Lee, J. H. (2018). A robust optimization for designing a charging station based on solar and wind energy for electric vehicles of a smart home in small villages. *Energies, 11*(7), 1728.
56. Mozafar, M. R., Moradi, M. H., & Amini, M. H. (2017). A simultaneous approach for optimal allocation of renewable energy sources and electric vehicle charging stations in smart grids based on improved GA-PSO algorithm. *Sustainable cities and society, 32*, 627-637.
57. Chen, W., Zhu, Y., Yang, M., & Yuan, J. (2017). Optimal site selection of wind-solar complementary power generation project for a large-scale plug-in charging station. *Sustainability, 9*(11), 1994.
58. Miri, I., Fotouhi, A., & Ewin, N. (2021). Electric vehicle energy consumption modelling and estimation—A case study. *International Journal of Energy Research, 45*(1), 501-520.
59. Akshay, K. C., Grace, G. H., Gunasekaran, K., & Samikannu, R. (2024). Power consumption prediction for electric vehicle charging stations and forecasting income. *Scientific Reports, 14*(1), 6497.
60. Armenta-Deu, C., Carriquiry, J. P., & Guzman, S. (2019). Capacity correction factor for Li-ion batteries: Influence of the discharge rate. *Journal of Energy Storage, 25,* 100839.
61. Nahavandi, A., Hagh, M. T., Sharifian, M. B. B., & Danyali, S. (2014). A nonisolated multiinput multioutput DC–DC boost converter for electric vehicle applications. *IEEE Transactions on Power Electronics, 30*(4), 1818-1835.
62. Bellur, D. M., & Kazimierczuk, M. K. (2007, October). DC-DC converters for electric vehicle applications. In *2007 Electrical Insulation Conference and Electrical Manufacturing Expo* (pp. 286-293). IEEE.
63. Saravanan, A., Chitra, L., Chandran, S. S., Aravind, B. S., Kumar, J. N., Jayaprakash, S., & Ramkumar, M. S. (2022, March). Distinguished DC-DC Converter for an Electric Vehicle. In 2*022 6th International Conference on Computing Methodologies and Communication (ICCMC)* (pp. 578-582). IEEE.
64. Jagadeesh, I., & Indragandhi, V. (2019, October). Review and comparative analysis on dc-dc converters used in electric vehicle applications. In *IOP Conference Series: Materials Science and Engineering* (Vol. 623, No. 1, p. 012005). IOP Publishing.
65. Electric Vehicle Socket Types [Accessed online: 17/06/2024]
66. Acharige, S. S., Haque, M. E., Arif, M. T., Hosseinzadeh, N., Hasan, K. N., & Oo, A. M. T. (2023). Review of electric vehicle charging technologies, standards, architectures, and converter configurations. *IEEE Access, 11,* 41218-41255.
67. Fischer, H. M., & Dorn, L. (2013). Voltage classes for electric mobility. *ZVEI-German Electr. and Electron. Manufacturers' Association.*
68. Wies, R. W., Johnson, R. A., & Agrawal, A. N. (2012). Energy-efficient standalone fossil-fuel based hybrid power systems employing renewable energy sources. *Fossil fuel and the Environment,* 121-142.

69. Penghou, Z., Yuexing, W., Haizhen, A., & Li, C. (2020, November). Tribology performance analysis of oil for wet drive axle. In *Journal of Physics: Conference Series* (Vol. 1676, No. 1, p. 012091). IOP Publishing.
70. Burton, T., Sharpe, D., Jenkins, N., & Bossanyi, E. (2001). Wind energy: handbook", John Wiley & Sons, Chichester.
71. How long last the electric vehicle charging? Energetic change. [Accessed online: 23/06/2024]
72. Charger Types and Speeds. U.S. Department of Transportation. [Accessed online: 21/06/2024]
73. Compare power curves of wind turbines. Wind-turbine-models.com [Accessed online: 21/06/2024]
74. Vestas V47. Wind-turbine-models.com [Accessed online: 21/06/2024]
75. New European Wind Atlas. [Accessed online: 21/06/2024]
76. Barclay, C. Wind Farms – Distance from housing. Library House of Commons. Science and Environment Section. SN/SC/5221. Last updated: 25/03/2011 Accessed online: 24/06/2024]
77. ROJEK, W. (1962). SIEMENS & HALSKE AKTIENGESELLSCHAFT BERLIN MUNCHEN ERLANGEN VOL. XXIX. 1962 NO. 2. *Siemens Review, 29*, 39.